Observations of Inertial Wave Events near the Continental Slope off Goban Spur

HENDRIK M. VAN AKEN, LEO R. M. MAAS, AND HANS VAN HAREN

Royal Netherlands Institute for Sea Research, Den Burg, Netherlands

(Manuscript received 6 May 2004, in final form 4 February 2005)

ABSTRACT

Near-inertial waves were observed during the Ocean Margin Exchange (OMEX-I) experiments with current meters over the continental slope near Goban Spur. The strongest inertial motion was observed in the bottom layer, about 50 m above the 1000-m isobath. There the waves were slightly (1.7%) superinertial and the bottom slope appeared to be critical for the near-inertial peak frequency, allowing the velocity vector to follow the sloping bottom. The vertical velocity component of this motion was responsible for the near-inertial spectral peak in the temperature spectrum, which was also observed in the bottom layer. Evidence was found supporting the speculative hypothesis that high-energy near-inertial wave events were produced during geostrophic adjustment in the variable deep eastern-boundary current over the slope near Goban Spur.

1. Introduction

For inertial oscillations or inertial waves that occur in the atmosphere and ocean, a strict balance is assumed between Coriolis acceleration and inertial (centrifugal) acceleration. Given the typical density stratification in the oceans the frequency of these oscillations (inertial or Coriolis frequency) forms the lower bound of the internal gravity wave band (Krauss 1966). Inertial waves, observed in a certain location in the ocean, are assumed to be generated either locally as a response to local forcing, or remotely at lower latitudes as internal waves with a frequency close to the inertial frequency at the observation site (Fu 1981). The local generation of inertial waves may be due to changes in the wind forcing at the sea surface (Ekman 1905; Pollard and Millard 1970, Alford 2001) or due to the geostrophic adjustment process of currents in the ocean interior (Rossby 1938; Gill 1982). According to the dispersion relation for inertiogravity waves,

$$m^2 = k^2 \frac{(N^2 - \omega^2)}{(\omega^2 - f^2)} \tag{1}$$

which gives the relation between horizontal and vertical wave numbers (k and m) and frequency ω, given the Brunt–Väisälä frequency N and Coriolis frequency f, the vertical scale of near-inertial gravity waves with a finite horizontal scale in a continuously stratified rotating ocean is assumed to be small (Krauss 1966; Gill 1982). The vertical wavelength $2\pi/m$ will approach zero in the limit case when ω approaches f. From observations with an acoustic Doppler current profiler (ADCP) nearby in the Bay of Biscay in the 600–1100-m depth interval, a typical vertical wavelength of near-inertial waves of 240 m was derived (van Aken et al. 2004, unpublished manuscript). Then intense near-inertial wave motion will probably lead to dissipation by shear instabilities, which transfer wave energy to turbulent motion. This turbulent motion may in turn support turbulent mixing, one of the main driving processes for the global oceanic deep circulation. A better understanding of near-inertial waves in the ocean may lead to enhanced insight into the large-scale oceanic circulation, which maintains a large part of the oceanic meridional heat transport (Peixoto and Oort 1992).

Ongoing research at the Royal Netherlands Institute for Sea Research deals with the structure of internal and near-inertial waves in the Bay of Biscay (e.g., van Haren et al. 2002; van Haren 2003). Recent analyses of ADCP measurements from the Bay of Biscay have shown that near-inertial waves near the continental slope may occur in relatively narrow beams (vertical scale $\approx$ 120 m) in the thermocline between depths of ~1000 and 500 m (van Aken et al. 2004, unpublished manuscript). Generally it is assumed for

Corresponding author address: Hendrik M. van Aken, P.O. Box 59, 1790 AB Den Burg Texel, Netherlands.
E-mail: aken@nioz.nl

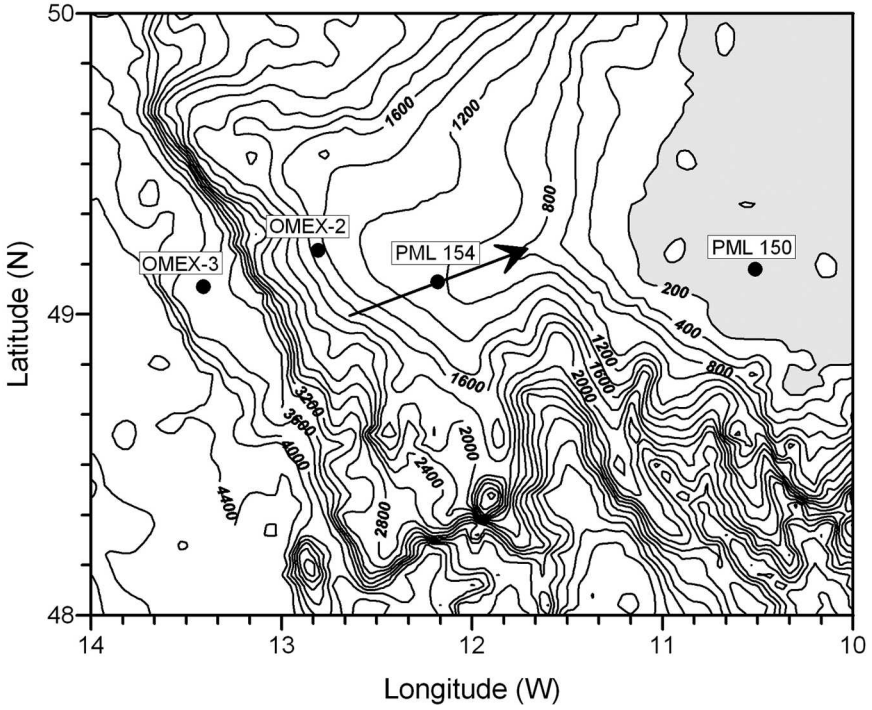

FIG. 1. Bathymetry of Goban Spur with isobaths every 200 m, based on the ETOPO-2 topographic dataset. The positions of the current-meter moorings deployed during the OMEX-I experiment are shown as black dots. The contour labels show the water depth in meters, and the continental shelf shallower than 200 m is shaded. The arrow at mooring PML 154 shows the direction of the near-inertial velocity component, correlated with the near-inertial temperature fluctuations.

the Bay of Biscay that most of the energy in the inertial wave band is generated near the sea surface as a result of varying wind forcing (e.g., Huthnance et al. 2001). However, upward as well as downward energy transport in the near-inertial and tidal internal wave beams were observed in the Bay of Biscay (Pingree and New 1991, 1995; van Aken et al. 2004, unpublished manuscript). Analysis of public current-meter data from the Ocean Margin Exchange (OMEX-I) research program, carried out near Goban Spur at the northwestern end of the Bay of Biscay, did show a maximum of near-inertial kinetic energy over the continental slope close to the 1000-m isobath (Pingree et al. 1999). Most kinetic energy at near-inertial frequencies was observed during a few short-term events. In this paper the observed temporal and spatial variation of the near-inertial waves near Goban Spur and related temperature variations will be presented in some detail. In the final chapter near-inertial wave propagation and generation are discussed. There evidence is presented that geostrophic adjustment of the deep eastern-boundary current along the continental slope may be the major source of kinetic energy at near-inertial frequencies.

2. The data

The multidisciplinary research program OMEX-I on the exchange of matter across the ocean margin, carried out near Goban Spur in the early 1990s, had a large physical subprogram (Huthnance et al. 2001). Current measurements with conventional paddle wheel current meters, fitted with a thermistor and pressure sensor were performed along a zonal section near 49°N, reaching from the continental rise at a depth over 3000 m to the continental shelf (Fig. 1). The data from these measurements have become public in 1997 (Antia 1997; Pingree 1997). The current-meter records are described in Table 1. The moorings represent from east to west respectively the continental shelf (PML 150), the continental slope (PML 154 and OMEX-2), and the continental rise (OMEX-3). The record length varied from only 2.5 months (PML 150) to over 2 yr (OMEX-3, 580 m). The records from OMEX-3 and OMEX-2 were based on a combination of several (3 or 4) successive deployment periods, while the records for PML 150 and PML 154 represented a single deployment period. The available sampling frequency generally was 24 cycles

TABLE 1. Summary of the OMEX-I current-meter observations over Goban Spur.

Mooring	Water depth (m)	Instrument depth (m)	Lat	Lon	Start date	End date
OMEX-3	3670	580	49°06′N	13°25′W	27 Jun 1993	29 Sep 1995
OMEX-3	3670	1490	49°06′N	13°25′W	27 Jun 1993	14 Jan 1995
OMEX-3	3670	3280	49°06′N	13°25′W	27 Jun 1993	14 Sep 1994
OMEX-2	1432	620	49°11′N	12°49′W	28 Jun 1993	28 Sep 1995
OMEX-2	1432	1070	49°11′N	12°49′W	28 Jun 1993	28 Sep 1995
PML 154	996	196	49°07′N	12°11′W	23 Jan 1994	7 Jun 1995
PML 154	996	496	49°07′N	12°11′W	23 Jan 1994	7 Jun 1995
PML 154	996	946	49°07′N	12°11′W	23 Jan 1994	7 Jun 1995
PML 150	142	30	49°09′N	10°31′W	15 Jun 1995	2 Sep 1995
PML 150	142	100	49°09′N	10°31′W	15 Jun 1995	2 Sep 1995

per day (cpd), although for one of the deployment periods of moorings OMEX-3 and OMEX-2, a sample frequency of 12 cpd was used. The original current-meter records gave the current speed in centimeters per second, the current direction relative to north, and the water temperature. The latter parameter was measured with a resolution of 0.02°C. From the current speed and direction the eastern and northern velocity components were calculated. Although not described on the OMEX data CD-ROM (Lowry et al. 1997), the power spectra of the current-meter data suggested that some data records were obtained by linear interpolation of the original data at discrete hours. This lowered the spectral density at frequencies over 8 cpd but did not effect the frequency range of the near-inertial wave band near 1.5 cpd.

3. Hydrographic setting

With RV *Pelagia* hydrographic surveys were carried out annually from 1993 to 1996 along a nearly zonal section close to the line of current-meter moorings shown in Fig. 1, which ran across the continental slope near Goban Spur. The sections contained 4–7 CTD stations each. At these stations the temperature and salinity profiles were measured from the sea surface to within 10 m from the bottom. Between 800- and 1100-m depth, in which range the maximum inertial motion was observed, a warm and saline core of the deep eastern-boundary current was found near the continental slope (Fig. 2). A second salinity maximum was observed further off the continental slope. This deep boundary current transports a core of Mediterranean Sea Outflow Water (MSOW) along the European continental slope (van Aken 2000). The annual mean current in the MSOW core, measured with the lowest current meter of mooring PML 154 (the dot in Fig. 2), was directed in a northwesterly direction, with a speed of 2.1 cm s^{-1}. At a depth of 1070 m the current meter of mooring OMEX-2 in the depth range of the MSOW core (the star in Fig. 2) showed an annual mean velocity of 5.4 cm s^{-1}, also directed to northwest. This speed difference agrees with a negative (anticyclonic) vorticity of the order of -10^{-6} s^{-1} at the levels of the MSOW core near the continental slope. Because of the thermohaline structure of the MSOW core and the geostrophic shear below that core, the isotherms and isopycnals are not horizontal and intersect the continental slope, with temperature increasing upslope. The horizontal temperature gradient at a depth of ~1000 m along the CTD and current-meter sections, nearly perpendicular to the continental slope, could be determined for each survey. The mean value of the gradient amounted to 0.007°C km^{-1} along the current-meter section. The presence and properties of the MSOW over the slope appeared to be strongly intermittent from survey to survey, leading to a relatively large standard deviation of the hori-

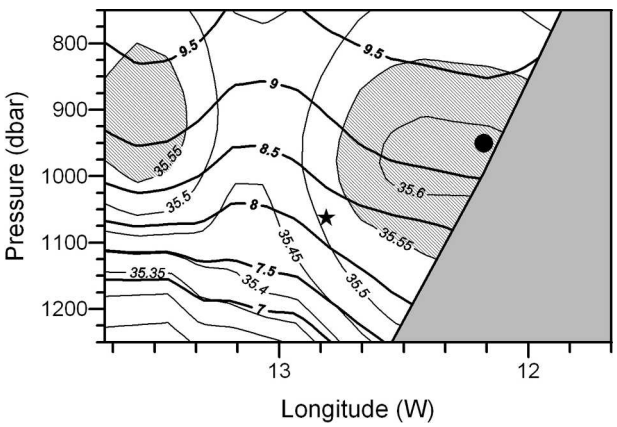

FIG. 2. Cross section of the mean distribution of temperature (thick lines and labels) and salinity (thin lines) based on hydrographic surveys carried out during the OMEX program in 1993, 1994, 1995, and 1996. The salinity maxima connected with the MSOW core are hatched. The dot indicates the position of the deepest current meter of mooring PML 154, and the star indicates the position of the deepest current meter of mooring OMEX-2.

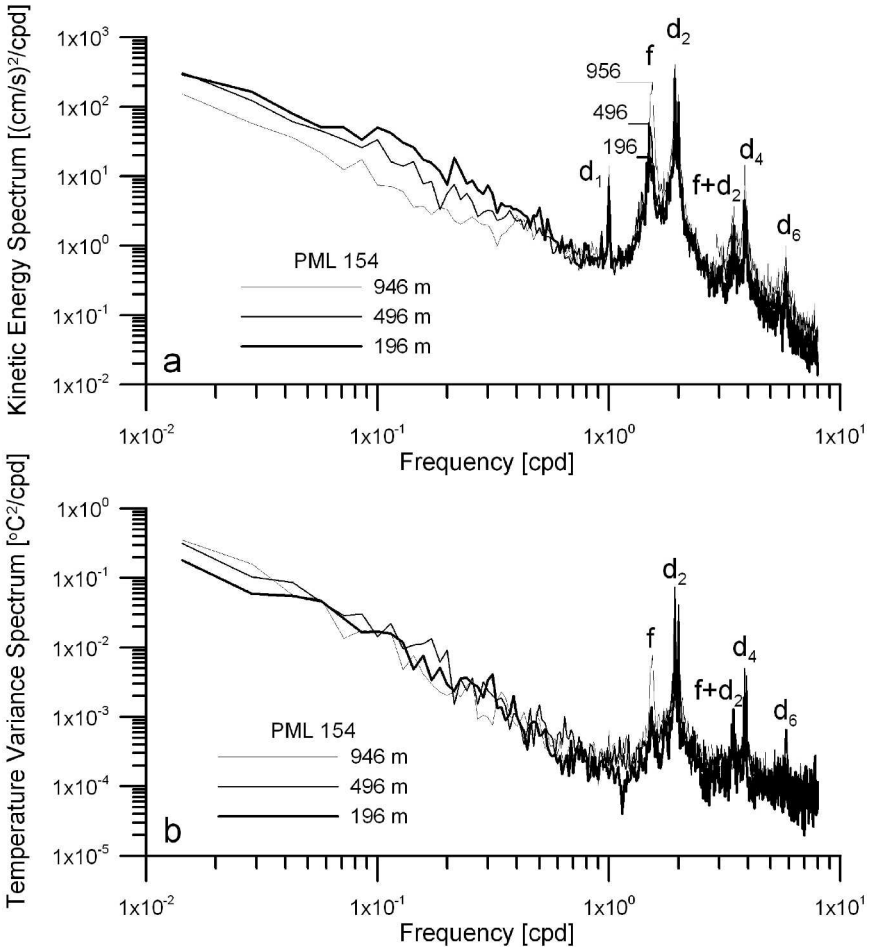

FIG. 3. Power spectra of the (a) kinetic energy and (b) temperature variance observed with the current meters of mooring PML 154. The spectral peaks show the near-inertial band (f), diurnal (d_1) and semidiurnal (d_2) tidal bands and higher tidal harmonics (d_4 and d_6) as well as the summed semidiurnal and inertial frequency band (f + d_2). The depth labels near the inertial peak in (a) show that the energy of the near-inertial band increases an order of magnitude toward the bottom. The inertial peak in the temperature spectrum at 956-m depth (b) is an order of magnitude higher than at shallower depths. The spectral estimates are averages of spectra for successive 70-day subperiods after detrending of these subperiods.

zontal gradient with a magnitude similar to the mean, 0.007°C km^{-1}. Near a depth of 1000 m the vertical gradient of the potential temperature showed a local minimum of 0.005 (±0.001)°C m^{-1}.

4. The near-inertial spectral peak

Representative examples of kinetic energy spectra are shown in Fig. 3a. These spectra were derived from the current observations carried out at mooring PML 154. Pingree et al. (1999) already presented a preliminary analysis of these spectra. All current-meter records showed kinetic energy spectra for the horizontal motion with peaks at semidiurnal (d_2 in Fig. 2a, formed by M_2 and S_2) and diurnal (d_1, mainly K_1) tidal frequencies as well as at the angular inertial or Coriolis frequency $f = 2\Omega \sin(\phi)$ (Ω is the angular frequency of the earth's rotation; ϕ is the geographic latitude), with occasionally peaks at higher tidal harmonic periods (~4 and 6 cpd). Similar to current-meter observations from the Bay of Biscay (van Haren et al. 2002, van Haren 2003; van Aken et al. 2004, unpublished manuscript) a spectral peak was also found near the sum frequency of the semidiurnal tides and the inertial frequency ($d_2 + f$). For the PML 154 mooring the height of the near-inertial peak significantly increased with a factor 12 from the shallowest current meter at a depth of 196 m to the deepest current meter at 946 m. The latter cur-

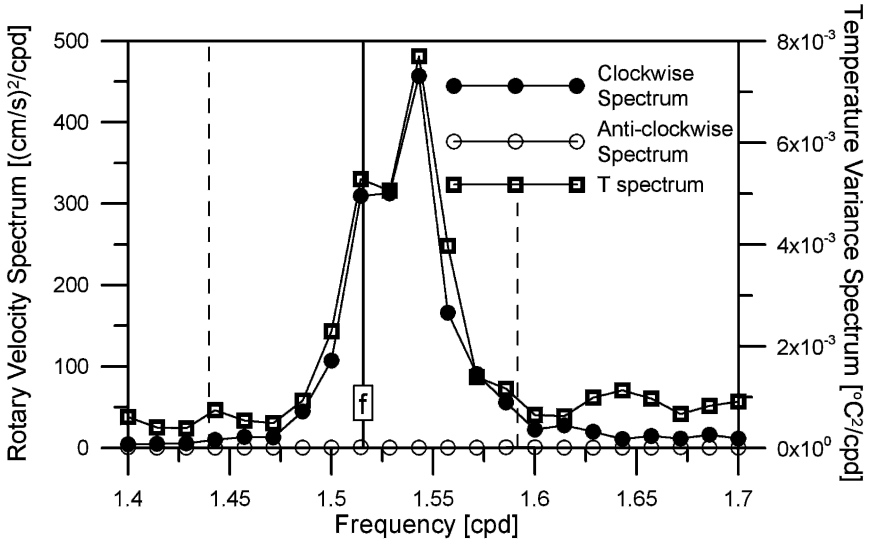

FIG. 4. A detailed graph of the near-inertial spectral peak of the rotary velocity spectrum and temperature spectrum from the near-bottom current meter at a depth of 946 m of mooring PML 154. The full vertical line marked f shows the local inertial frequency. The vertical dashed lines show the ±5% frequency boundaries of the near-inertial bandpass filter used in this study.

rent meter was located only 50 m above the bottom at the continental slope. The inertial peak from this instrument was by far the largest of all current observations carried out during the OMEX-I program.

The temperature variance spectrum of mooring PML 154 (Fig. 3b) showed peaks at semidiurnal and higher harmonic tidal frequencies. The temperature record from the near-bottom current meter also showed a significant near-inertial peak of at least about an order of magnitude larger than the temperature records from shallower levels or from other moorings. In the near bottom layer over the continental slope close to the 1000-m isobath the inertial motion apparently was quite vigorous, as was its interaction with the temperature field.

If we look in detail at the near-inertial peak of the rotary velocity spectrum and the temperature spectrum of the deepest current meter from mooring PML 154 (Fig. 4) it appears that the near-inertial spectral peaks for the clockwise rotating velocity component and for the temperature were found at a frequency, 1.7% above the inertial frequency f. The spectrum of the anticlockwise rotating velocity in the near-inertial wave band was several orders of magnitude (a factor of 330) smaller than the spectrum for the clockwise rotating velocity. About 70% of the kinetic energy and temperature variance in the near-inertial band was found at frequencies above the Coriolis frequency. This indicates that the motion in the near-inertial band still had an internal gravity wave character with a finite, although large vertical wavenumber and nonvanishing vertical velocity components (Krauss 1966; Gill 1982). The records from shallower current meters of mooring PML 154 (196 and 496 m) had a near-inertial peak in the frequency band of the local inertial frequency f, suggesting horizontal near-inertial motion at those levels.

One may question whether the observed superinertial spectral peak in Fig. 4 is an artifact of the vorticity in the background velocity field. However the annual mean velocities, measured at moorings PML 154 and OMEX-2 near 1000 m, suggest an anticyclonic background velocity field, which will lower the effective Coriolis parameter. If we can ignore the curvature of the flow field and the vertical shear between 1070 and 946 m, the annual mean vorticity ζ at these levels is on the order of $-0.01f$. That gives an effective Coriolis parameter of $f + 0.5\zeta = 0.995f$. This shift maintains and even strengthens the superinertial character of the spectral peak in Fig. 4.

To get insight into the spatial distribution of the near-inertial kinetic energy, KE_f, we have band-filtered the current-meter records with a bandpass filter adapted for the local inertial frequency. This filter was performed by a Fourier transformation of the raw data (velocity components u and v and temperature T) to frequency space, and a back transformation to a time series (u_f, v_f, T_f) for only the angular frequencies within 5% of f. The bandwidth of ±5% (dashed lines in Fig. 4) was chosen to ensure that nearly all energy of the near-

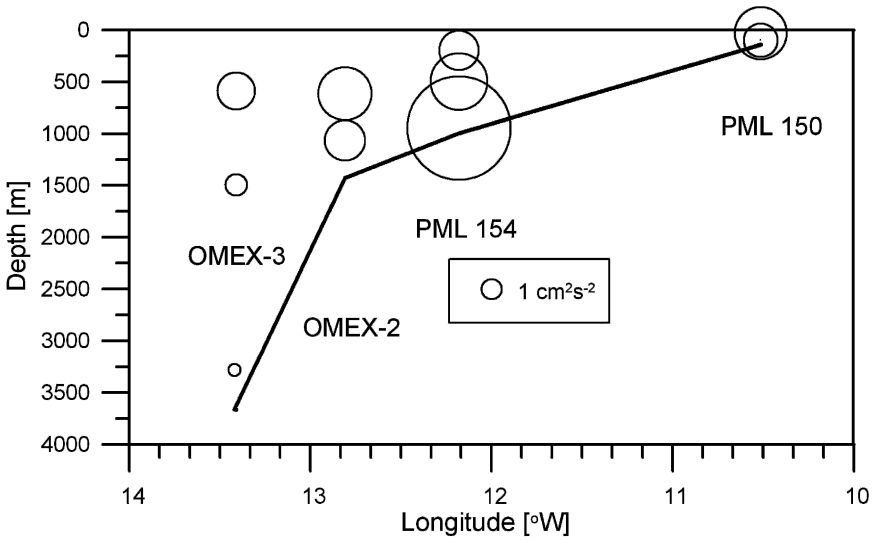

FIG. 5. The spatial distribution of the kinetic energy per kilogram in a frequency band within ±5% of the inertial frequency *f*. The surface of the circles is proportional to the near-inertial kinetic energy. The thick line represents the simplified bottom depth from the OMEX-3 mooring to the PML 150 mooring.

inertial wave band passed through, while no tidal contributions were incorporated. The resulting distribution along the current-meter section of the mean values of $KE_f = (u_f^2 + v_f^2)/2$ shows that indeed the most energetic near-inertial motion was observed at mooring PML 154 ($KE_f > 25$ cm^2 s^{-2}) at a depth of 956 m (Fig. 5). From there KE_f decreased upward. At the other moorings further downslope the highest KE_f values were found at the shallowest current meters, contrary to PML 154. There KE_f decreased down- and westward. Over the continental shelf the relatively high mean KE_f estimates from mooring PML 150 were based on only a few months of data and can hardly be compared with the longer-term estimates from the other moorings.

5. The temporal variability of inertial wave events

From the near-inertial bandpass-filtered current-meter data time series of the 48-h mean kinetic energy were derived for each current meter (Fig. 6). It appeared that that the near-inertial wave activity was a highly intermittent phenomenon with a few periods of high activity lasting about one week, while for most of the observational period KE_f was relatively low. The three dominant high KE_f events observed with the near-bottom current meter of mooring PML 154 are labeled 1–3. Event 1 had a KE_f magnitude of over 130 cm^2 s^{-2} at a depth of 956 m, while at the shallower current meters, the coincident KE_f peak magnitude only was about 10 cm^2 s^{-2}. For event 2, the near-bottom KE_f peak of over 180 cm^2 s^{-2} coincided with peaks of about 55 cm^2 s^{-2} at 496 and 196 m. During event 3, the KE_f peak at both 956 and 496 m was about 210 cm^2 s^{-2} while at 196 m its magnitude was 85 cm^2 s^{-2}.

About 2 weeks after event 2, observed at mooring PML 154, a high KE_f peak (~120 cm^2 s^{-2}) was observed at mooring OMEX-2, at a depth of 620 m, while no specific accompanying high KE_f event could be identified at mooring OMEX-3. However, the peak of event 3 at mooring PML 154 at 27 January 1995 was followed by a KE_f peak at OMEX-2 on 30 January and at OMEX-3 at 4 February, both times at a depth of about 600 m. One high KE_f event was observed coincident only at the western OMEX-2 and OMEX-3 (W1 in Fig. 5) but not at mooring PML 154. The peaks for event W1 were very outspoken in the current records from about 600 m, but hardly recognizable at deeper levels.

One can question how dominant the near-inertial waves are relative to the semidiurnal tides, which also showed a definite peak in the power spectrum. About 32% of the high-frequency total kinetic energy in the near-bottom layer of PML 154 at frequencies over 0.5 cpd could be attributed to near-inertial motion. A harmonic analysis showed that over the whole data record of the current meter at 956 m of mooring PML 154 the coherent M_2 harmonic tidal component represented only 24% of the high-frequency total kinetic energy at frequencies over 0.5 cpd. The semidiurnal frequency band with frequencies within 5% from the harmonic M_2 tidal frequency, which also contained the harmonic S_2

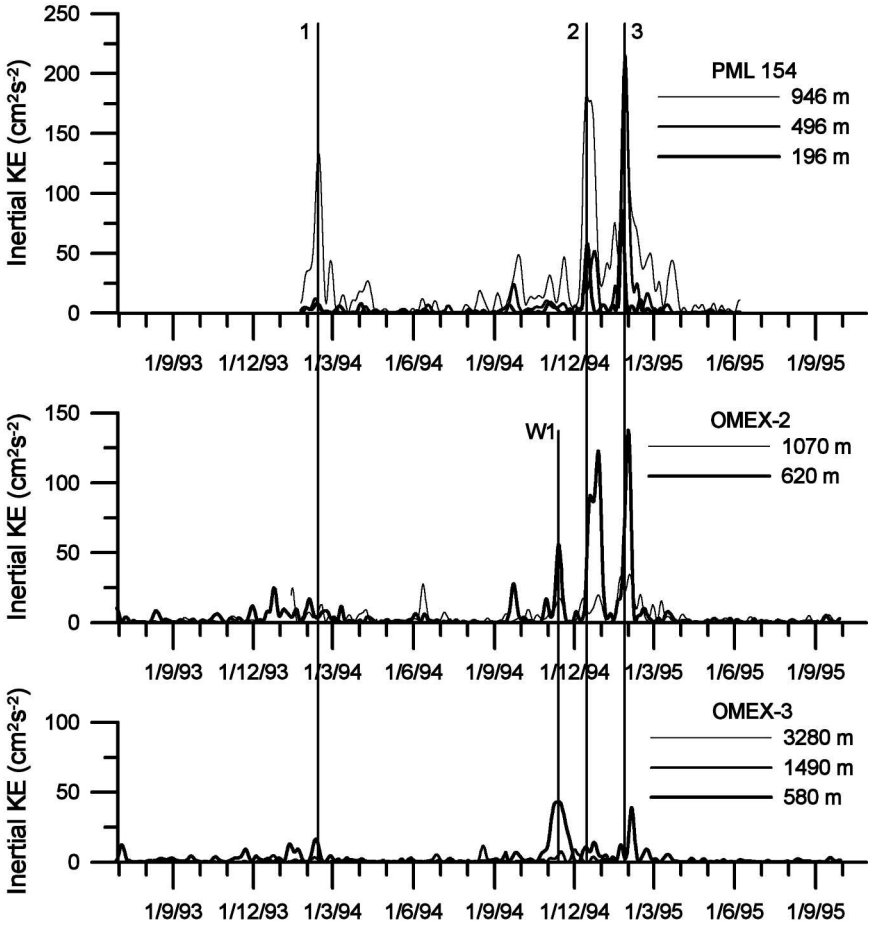

FIG. 6. Time series of the 48-h-averaged KE_f from the current records of moorings PML 154, OMEX-2, and OMEX-3. The results from mooring PML 150 are not shown, since they only lasted 2.5 months and did not coincide with the records of mooring PML 154. The three major inertial wave events at mooring PML 154 are indicated with vertical lines and numbered 1 to 3. The inertial wave event of 15 Nov 1994, observed only at the two westernmost moorings, is identified as W1.

tide as well as contributions from incoherent semidiurnal internal tides with random phase and amplitude, was responsible for 48% of the total KE_f. Apparently on average the near-inertial and tidal motions were of the same order of magnitude.

The comparison of the near-inertial band with the M_2 $\pm 5\%$ semidiurnal tidal band was also carried out for the high KE_f events 1 to 3 only. From this analysis it appeared that during these events on average 73% of the kinetic energy came from the near-inertial motion, while only 12% of the kinetic energy could be attributed to the semidiurnal tidal band. The near-inertial motion was the dominating factor determining the water velocity. A velocity vector diagram for event 3 (Fig. 7) illustrates this. The raw velocity vectors rotated in a clockwise direction, as can be expected for an inertial wave in the Northern Hemisphere. This rotation sense was encountered during all near-inertial events. In the example, given in Fig. 7, the mean kinetic energy connected with the near-inertial motion amounted to 150 $cm^2\ s^{-2}$, indicative for an inertial velocity amplitude of over 17 $cm\ s^{-1}$. During events 1 and 2, the corresponding KE_f values were 92 and 133 $cm^2\ s^{-2}$, respectively.

6. Temperature oscillations with near-inertial frequency

The temperature variance spectrum of the current meter from PML 154 at 956 m shows a strong and significant peak near the inertial frequency (Figs. 3b, 4). Given the properties of inertial waves in an f plane (Krauss 1966; Gill 1982), it is generally assumed that all near-inertial motion is dominantly horizontal. Such horizontal motion will not lead to temperature fluctua-

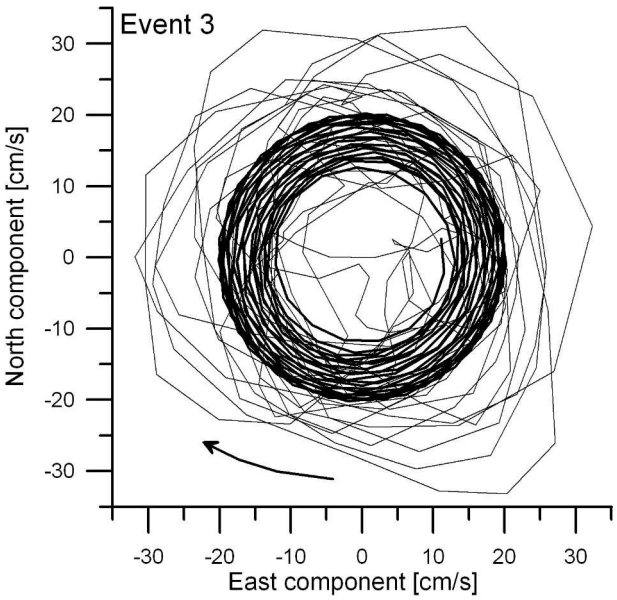

FIG. 7. The hodograph for the velocity vectors during event 3, measured in mooring PML 154 at 956-m depth. The arrow shows the rotation sense of the velocity vector. The thick line represents the bandpass-filtered near-inertial velocity; the thin line is the raw data high-pass filtered at frequencies above 0.5 cpd.

tions in a vertically stratified but horizontally homogeneous ocean. Therefore temperature fluctuations with near-inertial frequencies are generally attributed to either vertical motion of the sensor due to drag-induced mooring motion, or horizontal motion in a horizontal temperature gradient (Fu 1981). However, the mooring design of PML 154 was very tight, reducing the vertical motion of the uppermost current meter, 800 m above the bottom) to less than 1 m (standard deviation). With such a tight mooring it can be expected that the vertical motion of the current meter only 50 m above the bottom can be ignored.

The near-inertial spectral peak however was found at a frequency 1.7% above the local inertial frequency f (Fig. 4). Such a slightly superinertial spectral peak allows vertical motion in the near-bottom bottom current meter of mooring PML 154, with an aspect ratio α according to

$$\alpha = \frac{|w|}{|u|} = \frac{\sqrt{\omega^2 - f^2}}{\sqrt{N^2 - \omega^2}}, \tag{2}$$

where $|w|$ is the amplitude of the vertical velocity and $|u|$ is the amplitude of the cross-slope horizontal velocity, ω is the angular frequency of the wave, f is the Coriolis frequency, and N is the Brunt–Väisälä frequency (Gill 1982). The magnitude of the cross-slope depth gradient near mooring PML 154 approximately amounts to 100 m/10 km $= 10^{-2}$ (Fig. 1). With a near-inertial spectral peak at $\omega = 1.543(\pm 0.007)$ cpd, $f = 1.5156$ cpd, and $N = 39.2(\pm 1.3)$ cpd, the aspect ratio of the near-inertial motion, according to (2), will be $\alpha = 0.007(\pm 0.004)$, about equal to the bottom slope. If we use the effective Coriolis parameter due to the background vorticity near 1000 m, the estimate of α will increase to 0.008, but does not change the conclusion that within the accuracy of the estimates, the aspect ratio equals the bottom slope. The near-inertial peak frequency appears to be adapted to the local bottom slope, which is critical for the observed peak frequency, allowing near inertial motions to follow the sloping bottom. In a vertically stratified ocean such vertical near-inertial motion also may induce temperature oscillations in the near-inertial frequency band.

The temperature equation for near-inertial motion can be described as

$$\frac{\partial T}{\partial t} = -\mathbf{u} \cdot \nabla T = -u_x \frac{\partial T}{\partial x} - w \frac{\partial T}{\partial z}, \tag{3}$$

ignoring diffusion at the inertial time scales. Here u_x is the horizontal velocity component in the direction of the horizontal temperature gradient, x, while w is the vertical velocity component in the z direction. Given the large-scale temperature and salinity distribution due to the presence of the MSOW core over the continental slope (Fig. 2), the direction of the horizontal gradient (x) is expected to be the cross-slope direction.

Close to the bottom of the continental slope (50 m) the particle motion will be parallel to the sloping bottom, according to

$$w = -u_x \frac{\partial h}{\partial x}, \tag{4}$$

where now u_x is the velocity component in the direction x of the gradient of the bottom depth, h. The combination of (3) and (4) leads to

$$\frac{\partial T}{\partial t} = -u_x \frac{\partial T}{\partial x} + u_x \frac{\partial h}{\partial x} \frac{\partial T}{\partial z}. \tag{5}$$

Equation (5) suggests that a "strong" linear correlation can be expected between the time derivative of the temperature and the horizontal velocity component in the cross-slope direction. x. Perpendicular to that x direction the correlation will be zero. We have analyzed the relation between the inertial band passed temperature derivative and the bandpassed velocity component for the lowest current meter of PML 154. By means of a linear regression analysis the correlation between the temperature derivative and the velocity component in a variable horizontal direction was determined. The

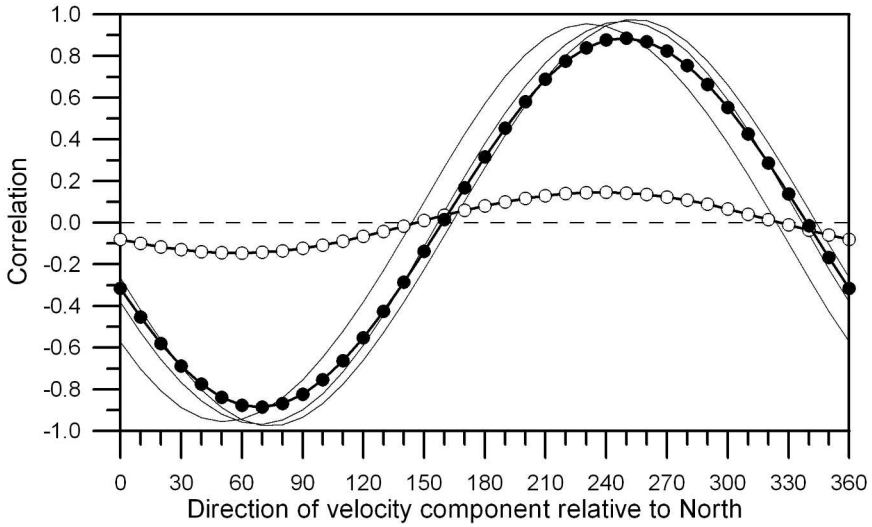

FIG. 8. Linear correlation between the time derivative of the near-inertial bandpass-filtered temperature and horizontal velocity component in variable directions relative to north. The black symbols represent the correlation derived from the whole 501-day current-meter record from the current meter of mooring PML 154 at 946-m depth. The thin lines give the correlation derived for the three high KE_f events measured with the same current meter. The open symbols show the correlation derived for the PML 154 current meter at 496-m depth.

maximal negative correlation coefficient for the whole record of over 500 days was found to be −0.89 when u_x was the velocity component in a direction of 69° relative to north (Fig. 8, black symbols). This direction appears to be the direction of the local bottom slope near mooring PML 154 (the arrow in Fig. 1). That is also the direction where the horizontal velocity component is expected to be correlated with the vertical component, with an aspect ratio according to (2). For the whole record the near-inertial waves contributed 15% of the total high frequency (>0.5 cpd) temperature variance. During high-KE_f events 1 to 3 the near-inertial temperature variability was also strongly enhanced. A regression analysis for these events separately showed correlations between the bandpass-filtered temperature derivative and the velocity component in a mean direction of 65° relative to north of over 0.95 (Fig. 8, thin lines). During the events 34% of the total high-frequency (>0.5 cpd) temperature variance could be explained from near-inertial waves in a temperature gradient.

With knowledge of the bottom slope, mean vertical temperature gradient and horizontal temperature gradient in the cross-slope direction (69°) from the repeated hydrographic surveys, we have derived an approximation of the right-hand side of (5) in the near-inertial wave band from the near-inertial velocity components and compared it with the observed time derivative which gave a very good fit, as is illustrated for the first week of event 2 (Fig. 9). It appeared that 98% of the observed temperature variance in the near-inertial wave band could be explained from the vertical motion in a stratified ocean, allowed by the superinertial peak frequency. Only 2% of the variance was generated by the near-inertial horizontal motion in the horizontal temperature gradient.

For the current meter of mooring PML 154 at 496-m depth a maximum negative correlation between u_x and $\partial T/\partial t$ of only –0.15 was found (Fig. 7, open symbols), implying that only 2% of the observed high frequency temperature change could be explained by the correlation with a near-inertial velocity component. That agrees with the fact that higher in the water column, at both 196 and 496 m the near-inertial peak was found in the frequency band closest to the local inertial frequency (1.5143 and 1.5156 cpd, respectively). At those levels the near-inertial motion therefore was approximately horizontal, according to (2).

7. Discussion

From our analysis of the near-inertial motion over the continental slope near Goban Spur, it has become clear that the strongest near-inertial motion was found in the bottom layer near the 1000-m isobath, represented by the lowest current meter from mooring PML 154. The near-inertial motion appears to make the largest (quasi-) periodic contribution to the high-frequency

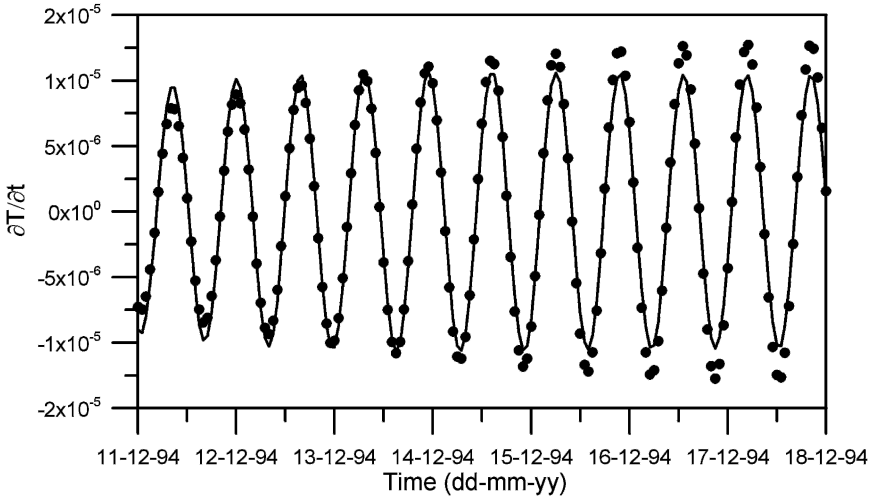

FIG. 9. A plot of the near-inertial temperature derivative (dots), observed 50 m above the bottom in mooring PML 154 during part of event 2. The full line represents the reconstruction of the temperature derivative with the right-hand side of (4), using the near-inertial u_x time series in a direction of 69° and estimates of the vertical and horizontal components of the temperature gradient as well as the bottom slope.

(>0.5 cpd) kinetic energy, even larger than the coherent M_2 harmonic tidal contribution. A large contribution to the near-inertial kinetic energy in all current-meter records appears to come from only a few high-energy events during which the semidiurnal tides appear to contribute less than 10% to the total kinetic energy. Sometimes a high KE_f event at mooring PML 154 occurred at all observational levels (events 2 and 3), although with varying EK_f ratios. This coincidence between the different levels of mooring PML 154 suggests a large vertical scale for these near-inertial events. But event 1 was only observed by the lowest current meter in PML 154, event 2 at PML 154 and the uppermost current meter at OMEX-2, while event W1 was only observed at the more western OMEX-2 and OMEX-3 locations, and a less intense event near 15 June 1994 only at the shallowest current meter of OMEX-2. While events 2 and 3 occurred at all three levels of PML 154 more or less synchronously, a delay of 14 days between PML 154 and OMEX-2 was observed for event 2. This delay agrees with a westward propagation velocity of about 4 cm s^{-1}. The group velocity by which internal wave energy is propagated can be derived from the dispersion relation (1). The horizontal and vertical components of the group velocity, which equal $\partial\omega/\partial k$ and $\partial\omega/\partial m$, respectively, can be derived from (1) as a function of m and ω, given N and f. For the horizontal group velocity of internal waves with a frequency of $1.017f$ at and a mean Brunt–Väisälä frequency (39.2 cpd) as found between 800 and 1100 dbar from the CTD surveys, a vertical wavelength of the waves of about 500 m (horizontal wavelength 71 km) is required to match that propagation velocity. If the vertical wavelength is about half of that, as observed in the nearby Bay of Biscay (van Aken et al. 2004, unpublished manuscript) the wave energy is propagated too slow by a factor of 2. Event 3 appeared to propagate with a mean westward velocity of about 13 cm s^{-1}, which caused a delay of 8 days between PML 154 and OMEX-3. The magnitude of this propagation velocity seems to be unrealistically high however, requiring a vertical wavelength of 1625 m (horizontal wavelength 232 km), deeper than the local water depth between PML 154 and OMEX-2, which casts doubt on the interpretation of the peaks in KE_f at OMEX-2 and OMEX-3 in terms of simple horizontal propagation of near-inertial motion from PML 154. The occurrence of near-inertial motion over the continental slope near Goban Spur appears to be mainly intermittent, not only in time but also in space.

The observed temperature variations with near-inertial frequency in the near-bottom layer of PML 154 appear to be related to the existence of vertical velocity in the near-inertial wave band, generated by motion parallel to the sloping ocean floor at the continental slope. The existence of vertical motion in the near-inertial wave band requires a frequency above the local Coriolis frequency. The existence of such vertical motion is also suggested by the spectral peak at a 1.7% superinertial frequency. At shallower levels this effect is much less. While at the deepest current meter at PML 154 the regression of the near-inertial bandpass-filtered

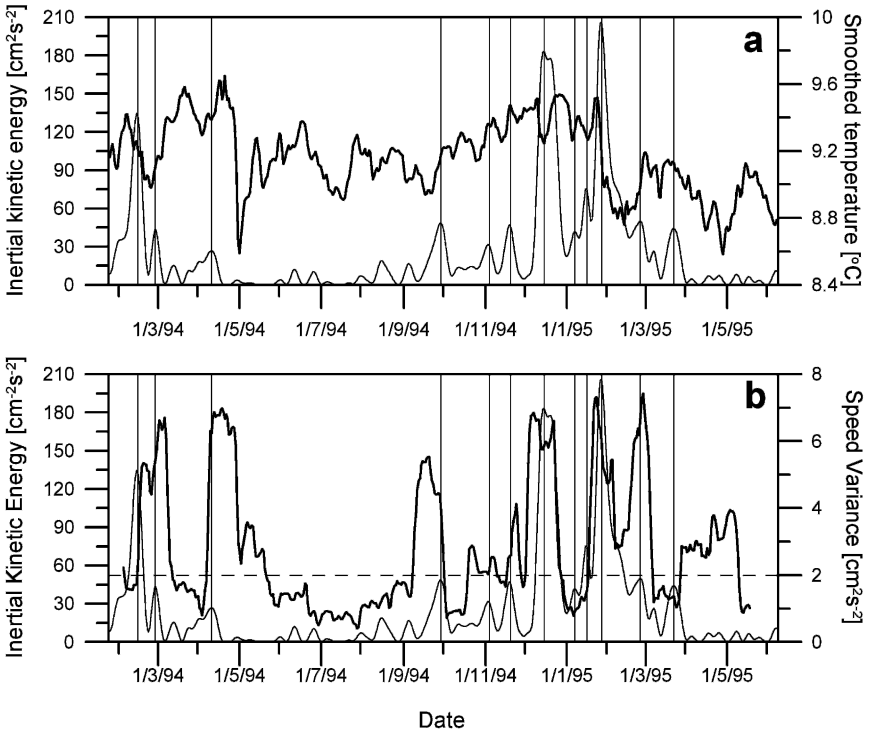

FIG. 10. A time series plot of the 48-h-averaged KE_f (thin line) and (a) the temperature (thick line) for the deepest current meter at 946 m from mooring PML 154 or (b) the 20-day variance of the 48-h-average current speed. The vertical lines show all KE_f events with a value above 25 $cm^2\ s^{-2}$. The horizontal dashed line in (b) shows the speed variance level of 2 $cm^2\ s^{-2}$.

temperature and a horizontal velocity component could explain 79% (correlation squared) of the temperature variance, the similar regression for the intermediate current meter at 495 m explained only 2% of the near-inertial temperature variance. At the latter level apparently high-frequency vertical motions at near-inertial frequencies were very weak, relative to 50 m above the bottom. This agrees with the near-inertial spectral peak in the inertial spectral band for the shallower current meters.

The apparent intermittency of EK_f both in time and space is not consistent with a large-scale wind forcing at the sea surface in synoptic weather systems, which have horizontal scales of 500–1000 km. The intermittency indicates that the observed deep high inertial energy events either are generated very locally in time and space, while decreasing strongly as the inertial energy spreads, or they propagate through the eddy-containing and seasonally varying ocean as relatively narrow but varying wave beams, which only occasionally hit the current meters. But not all successions of high KE_f events can be ascribed to wave propagation with the group velocity, since that occasionally would require unrealistically large vertical scales of the near inertial waves. Note also that near the bottom at mooring PML 154 the energy of the near-inertial f + 1.7% peak will be transported in the direction of the critical slope of internal waves at that frequency, that is parallel to the sloping bottom. This hinders a direct link between KE_f events near the bottom at mooring PML 154 and events observed at other moorings or shallower levels.

One may speculate on the source of the near-inertial kinetic energy. The high mean KE_f, observed in the near-bottom layer of PML 154, as well as the very high magnitude of the high KE_f events observed there, suggest that either this location is close to a site where inertial waves are preferentially generated, or that this location is close to an attractor where near-inertial wave beams converge (Maas 2001). Generation of inertial motion in the bottom layer near PML 154 will probably be due to geostrophic adjustment (Rossby 1938; Gill 1982) instead of variable wind forcing at the sea surface. Along the continental slope a northward subsurface boundary current from the Gulf of Cadiz to the Porcupine Sea Bight north of Goban Spur transports, between approximately 500- and 1500-m depth, warm and saline MSOW northward (Fig. 2). Following the 1000-m isobath, the deep flow has to make approximately a U-turn near Goban Spur (see Fig. 1), which possibly enhances the forma-

tion of instabilities in the deep boundary current. Instabilities in the current may lead to geostrophic adjustment processes, which in their turn may generate near-inertial waves. OMEX-2 and OMEX-3, farther west off the continental slope, are apparently out of the direct influence of the boundary current. They have the maximum mean EK_f at the shallowest current meters, located in the permanent thermocline. Inertial waves generated by variable wind forcing may be more important there.

It can be expected that high-KE_f events, if caused by geostrophic adjustment of a varying deep eastern-boundary current, will be correlated with changes in current speed and temperature which reflect changes in the northward transport of warm MSOW. The location where the geostrophic adjustment occurs and near-inertial waves are generated, as well as the location of the largest temperature and velocity changes connected with a changing flow, are unknown and do not necessarily coincide with one of the current meters. However, we may take the low-pass filtered temperature and the variance of the low-pass filtered current speed at 946 m at mooring PML 154 as a proxy for the flow state of the deep boundary current. These parameters show a considerable variability on time scales of a week to a year (Fig. 10, thick lines). The influence of the annual variation of the current velocity (Pingree et al. 1999) can probably be ignored, since it only contributes 0.01 $cm^2\ s^{-2}$ to the 20-day variance of the current speed, which has a typical value of 3 $cm^2\ s^{-2}$. If one compares the proxies with the KE_f record at the same position (Fig. 10, thin line) it becomes clear that not every strong change in background temperature is followed within a short time by a high-KE_f event. However, of the 12 events with $KE_f > 25\ cm^2\ s^{-2}$ (vertical lines in Fig. 10a), 11 events occurred within a few days after a strong change (either positive of negative) in temperature commenced. Out of the 12 high KE_f events, 10 took place during periods with high current speed variance (above 2 $cm^2\ s^{-2}$, the dashed line in Fig. 10b). These coincidences support the idea of a relation between current changes and the generation of near-inertial waves. Of course this is not a complete proof of a direct link between the occurrence of deep high-KE_f events and instabilities of the deep boundary current, but at least it suggests a future line of research on the generation of near-inertial waves over the continental slope. Another research line will have to deal with the propagation and dissipation of near-inertial kinetic energy, which may establish the importance of inertial motion for the maintenance of turbulent mixing near the continental slope.

Acknowledgments. The current-meter data used in this paper were obtained from the OMEX-I data CD-ROM. Doctors A. Antia (GEOMAR, Kiel) and R. Pingree (PML, Plymouth) were the principal investigators responsible for the collection and initial processing of the current-meter data. The OMEX-I program was funded by the EU under the second phase of the European Union Marine Science and Technology (MAST) program.

REFERENCES

Alford, M. H., 2001: Internal swell generation: The spatial distribution of energy flux from the wind to mixed layer near-inertial motions. *J. Phys. Oceanogr.,* **31,** 2359–2368.

Antia, A., 1997: *OMEX I Data Set*. CD-ROM electronic publication, British Oceanographic Data Centre.

Ekman, V. W., 1905: On the influence of the earth's rotation on ocean currents. *Ark. Mat. Astron. Fys.,* **2,** 1–52.

Fu, L.-L., 1981: Observations and models of inertial waves in the deep ocean. *Rev. Geophys. Space Phys.,* **19,** 141–170.

Gill, A. E., 1982: *Atmosphere–Ocean Dynamics*. Academic Press, 662 pp.

Huthnance, J. M., and Coauthors, 2001: Physical structures, advection and mixing in the region of Goban Spur. *Deep-Sea Res.,* **48B,** 2979–3021.

Krauss, W., 1966: *Interne Wellen*. Gebrüder Borntraeger, 248 pp.

Lowry, R. K., R. M. Downer, and Z. Loncar, 1997: *OMEX I Data Set Users' Guide, OMEX I Data Set*. CD-ROM electronic publication, British Oceanographic Data Centre.

Maas, L. R. M., 2001: Wave focusing and ensuing mean flow due to symmetry breaking in rotating fluids. *J. Fluid Mech.,* **437,** 13–28.

Peixoto, J. P., and A. H. Oort, 1992: *Physics of Climate*. American Institute of Physics, New York, 520 pp.

Pingree, R., 1997: *OMEX I Data Set*. CD-ROM electronic publication, British Oceanographic Data Centre.

——, and A. L. New, 1991: Abyssal penetration and bottom reflection of internal tidal energy in the Bay of Biscay. *J. Phys. Oceanogr.,* **21,** 28–39.

——, and ——, 1995: Structure, seasonal development and sunglint spatial coherence of the internal tide on the Celtic and Armorican shelves in the Bay of Biscay. *Deep-Sea Res.,* **42A,** 245–284.

——, B. Sinha, and C. R. Griffiths, 1999: Seasonality of the European slope current (Goban Spur) and ocean margin exchange. *Cont. Shelf Res.,* **19,** 929–975.

Pollard, R. T., and R. C. Millard, 1970: Comparison between observed and simulated wind-generated inertial oscillations. *Deep-Sea Res.,* **17,** 813–821.

Rossby, C. G., 1938: On the mutual adjustment of pressure and velocity distributions in certain simple current systems, II. *J. Mar. Res.,* **1,** 239–263.

van Aken, H. M., 2000: The hydrography of the mid-latitude Northeast Atlantic Ocean: II, The intermediate water masses. *Deep-Sea Res.,* **47A,** 789–824.

van Haren, H., 2003: On the polarization of oscillatory currents in the Bay of Biscay. *J. Geophys. Res.,* **108,** 3290, doi:10.1029/2002JC001736.

——, L. Maas, and H. M. van Aken, 2002: On the nature of internal wave spectra near a continental slope. *Geophys. Res. Lett.,* **29,** 1615, doi:10.1029/2001GL014341.